HiSST: 3rd International Conference on
High-Speed Vehicle Science Technology
14 -19 April 2024, Busan, Korea

Investigation of Aerodynamic Coefficient and Compressibility Effect of AGARD-B Model Based on Wind Tunnel Experiment and CFD Simulation

Hung-Yen Chou[1], Hsien-Hao Teng[2]

Abstract

In aerodynamics, wind tunnel testing is a widely used technique to provide experimental verifications of flow properties and corresponding characteristics. To maintain the accuracy of the data, it's important to calibrate the force and moment coefficients with a standard model to establish confidence in the data accuracy and flow quality. In this research, the test was carried out in the 4ft × 4ft tri-sonic wind tunnel of ASRD-NCSIST, applying the AGARD-B standard calibration model. The aerodynamic loads were measured by a six-component internal force balance at angles of attack varying from -4 to 12 degrees and Mach numbers from 0.4 to 4.5. Additionally, the total pressure, static pressure of the wind tunnel, and base pressure of the model were measured.

While wind tunnel experiments are important and widely used, there are some disadvantages such as complicated and time-consuming experiment design and the inconvenience of carrying out flow visualization in supersonic conditions. Therefore, computational fluid dynamic (CFD) simulation technology can be applied to complement the disadvantages of experimentation. If the aerodynamic coefficients measured from the experiment match those calculated from simulation within certain tolerance range, we can be more confident that the simulation is reasonable and reliable. This way, the flow field can be simulated to observe aerodynamic phenomena such as vortex or wake.

The aerodynamic coefficients of the AGARD-B model are measured in the wind tunnel. According to the definition, the total drag is the sum of forebody drag and base drag. To calculate the forebody drag precisely, the base pressure data must be accurately measured. In this test, the base drag was found to be apparently much higher than in other tests performed by the Arnold Engineering Development Center (AEDC) in the USA and the Advisory Group for Aerospace Research and Development (AGARD) in Europe. To correct this error, the static pressure data at the model support position must be measured by a static-pressure probe. After re-calculation, both the base drag and forebody drag were found within the region offered by AGARD publications. Furthermore, the coefficient is validated against the result from CFD Simulation, and the data are within the tolerance range. The numerical simulations were performed using Fluent and an unstructured mesh with near-wall treatment and the κ-ω SST turbulence models. Proceeding to the next step, the flow topologies over the AGARD-B model at Mach 0.80 and 0.95 are investigated. According to the experimental data and flow-field simulation, vortex bursting occurs along with the decrease of lift. When vortex bursting happens, there is a recovery shock located between the primary and secondary vortex, and a lack of shock is observed between the wing and vortex. As the angle of attack or Mach number increases, the vortex bursting location would be different, which needs to be replicated in the wind tunnel using additional equipment if possible.

For wind tunnel calibration, the main purpose of the AGARD-B standard calibration model is to measure the aerodynamic loads and compare them to previous data or reports. If the location of vortex bursting

[1] *Aeronautical Systems Research Division, National Chung-Shan Institute of Science and Technology, No. 300-5, Ln. 277, Xi'an St., Xitun Dist., Taichung City 407104, Taiwan (R.O.C.), e31xb07@gmail.com*

[2] *Aeronautical Systems Research Division, National Chung-Shan Institute of Science and Technology, No. 300-5, Ln. 277, Xi'an St., Xitun Dist., Taichung City 407104, Taiwan (R.O.C.), d515484@ncsist.org.tw*

and vortex separation at different Mach numbers can be replicated, this could be used as additional comparison criteria for wind tunnel calibration.
Keywords: *Tri-sonic wind tunnel, AGARD model, Compressibility effect, CFD, Vortex bursting*

Nomenclature

α	Angle of attack [Degree]
b	Wing span [m]
c	Mean aerodynamic chord [m]
S	Reference area [m^2]
AOA	Angle of attack
MAC	Mean Aerodynamic Chord
C_L	Lift coefficient
C_m	Pitch moment coefficient

1. Introduction

The purpose of wind tunnel tests is to create a controllable flow condition and verify the aerodynamic characteristics or flow structure of flight vehicles. To maintain data accuracy, the calibration procedure with a standard model is essential for determining overall data quality, providing engineers or end customers with assessment documents. The AGARD-B model, designed by the Advisory Group for Aerospace Research and Development (AGARD) in Europe, has become the standard for wind tunnel calibration [1], and a number of publicly available tests have been performed[2][3]. This calibration process is conducted regularly for the tri-sonic wind tunnel in Taiwan, and the results are compared with those published by the Arnold Engineering Development Center (AEDC) in the USA and AGARD in Europe. Furthermore, CFD simulation has been applied to observe the flow structure at Mach 0.8 and 0.95.

Under these flow conditions, the effect of shockwaves does matter. Because the AGARD-B model features a 60° biconvex wing, the flow region manifests itself according to the Mach number and angles of attack normal to the wing's leading edge. The Stanbrook-Squire line [4] separates flows with attached leading edges from those with separated flow leading edges. In the leading edge separation region, the Mach number normal to the leading edge is less than one, and there is a secondary attached vortex and a prevalent centreline shock region at higher angles of attack normal to the leading edge. Tuling et al. [5] studied the centreline shock region and identified a lambda shock in the region of the secondary vortex at subsonic speeds. The structure and mechanism of vortex bursting have been intensively studied in the past, and the bursting modes have been identified, including bubble and spiral modes [6] [7]. The unsteady or periodic flow aspects of vortex bursting have also been studied, including surface pressures, turbulence intensity, spectral density, frequency content, and their effect on downstream surfaces [8]. The study of vortex breakdown is not merely an observation of simple flow structures but also an exploration of the potential to control or enhance other desirable effects, and the control mechanisms have been widely studied, including suction, blowing down, or jets at the trailing edge [9].

2. Experimental apparatus and Numerical Simulations

The experimental facilities include a tri-sonic wind tunnel, force measurement and pressure measurement systems, calibration processes. And experiment results are presented as follows.

2.1 Tri-sonic wind tunnel

All the experiments were performed in a blow down & open circuit tri-sonic wind tunnel at NCSIST, as illustrated in Fig.1, with test section area 1.2m × 1.2m, speed range from Mach 0.4 to 4.5, total volume of gas tank 1500m^3, maximum storage pressure level 600 psia, and the normal test temperature 37°C.

Fig. 1 Tri-sonic wind tunnel in NCSIST

2.2 AGARD-B standard model

The AGARD calibration model B was originally designed by the AGARD committee for the calibration of supersonic wind tunnels and is also used for the calibration of transonic wind tunnels [1]. The dimensions of the model are defined in Fig. 2, featuring a configuration that combines an ogive-cylinder body with a delta wing shaped as an equilateral triangle, with a span four times the body diameter. The body is a cylinder of revolution with an ogive nose. To adapt to the dimensions of the test section, the diameter of the body is 7.62 cm, as shown in Fig. 3.

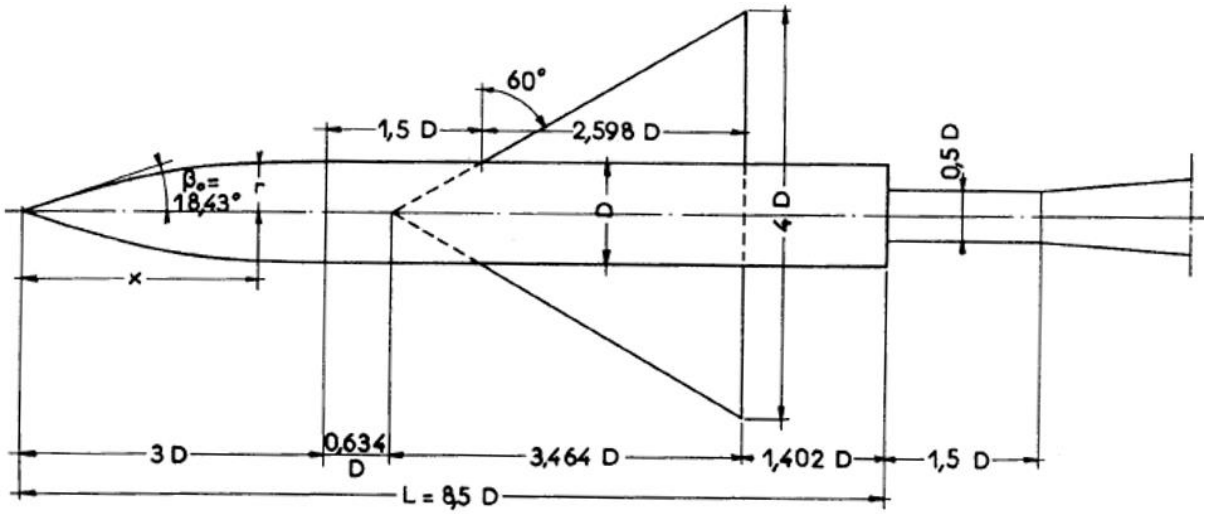

Fig 2 Model and support dimension (D: diameter)

Fig.3 AGARD-B calibration model

2.3 6-components force balance

In this test, the ABLE MK-VI 6-component internal force balance was used. The maximum load and calibration range are listed in Table 1, with related parameters provided in Table 2. Based on the calibration results, the maximum error for each component is less than 0.5% of the maximum load.

The data from the force balance can be transformed into parameters based on the body axis or stability axis for further analysis needs.

Table 1 Maximum load and calibration range of balance

Item	Max. load	Calibration range	Max. error	
			Value	(%)
Normal force (N1)	±450 kg	-250~250 kg	0.039 kg	0.0171
Normal force (N2)	±450 kg	-300~300 kg	0.039 kg	0.0174
Side force (S1)	±220 kg	-100~100 kg	0.0047 kg	0.0194
Side force (S2)	±220 kg	-100~100 kg	0.0024 kg	0.0104
Axial force (AF)	±60 kg	-30~30 kg	0.0051 kg	0.0188
Rolling moment (RM)	±12 kg-m	-6~6 kg-m	0.000036 kg-m	0.0053

Table 2 Parameters of force balance and model

Item	Parameters
Reference area(S)	0.0402 m2
Wing span(b)	0.3048 m
Mean aerodynamic chord(c)	0.1760 m

3. Numerical Simulations Setup

The current study involved a numerical investigation of the aerodynamics on the AGARD-B model using a commercial computational fluid dynamics (CFD) solver. We used FLUENT to solve the steady, compressible Reynolds-Averaged Navier-Stokes (RANS) equations with the Shear Stress Transport (SST) k-ω turbulence model. The SST k-ω turbulence model is capable of predicting the flow separation process with higher accuracy and is therefore preferred for the present case study. Near-wall mesh sizes are arranged appropriately to resolve the boundary layer velocity profile within the viscous sublayer. Low Reynolds number flow within the viscous sublayer always exists, even for high Reynolds number main flow. As the near-wall grid structures are prepared with the intention to capture the viscous sublayer velocity profile, a low (near-wall cell) Reynolds number solution method is selected accordingly. The near-wall characteristic coordinate, y+, is a very important parameter for resolving the features of the boundary layer. The geometry was modeled using ANSYS SpaceClaim software, associated with FLUENT. A mesh consisting of Poly-Hex cells was constructed using 5,500,801 cells. The mesh and prism layers around the model are shown in Fig. 4. The y+ was checked to ensure it was of the order of 0.5 and less than 1, as shown in Fig. 5.

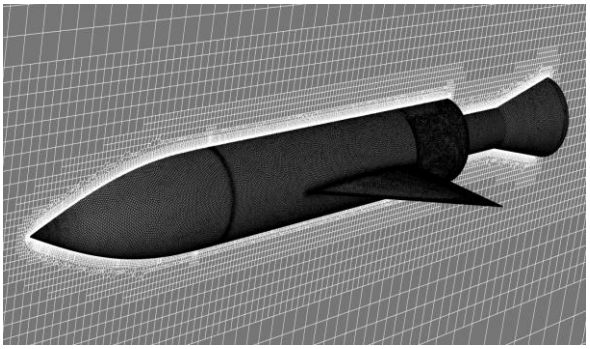

Fig. 4 Prism cells around the AGARD-B

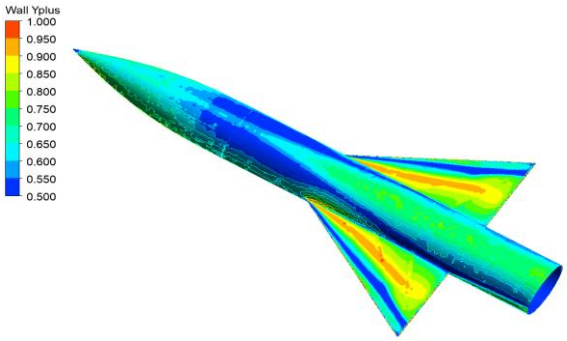

Fig. 5 AGARD-B y+ distribution

4. Result and Discussion

The measurement data consists of aerodynamic properties, including variations in lift coefficients, for which further comparison with reference and CFD results is described as follows.

4.1 Aerodynamic coefficients from experiment

To examine the quality of experimental data, the aerodynamic coefficient comparison results of reference and experiment at Mach 0.8 and 0.95 are illustrated in Figs. 6 and 7. For the relationship between the lift coefficient (C_L) and angle of attack (AOA), the curve is linear. Although the lift coefficient is not identical to that from the reference test results and has a slightly higher slope, the trends match each other without significant differences. For the relationship between the pitch moment coefficient (C_m) and AOA (Ref. point is at 50% MAC), the trend matches without significant difference as well. Additionally, the slope of the lift coefficient and pitch moment coefficient at Mach 0.95, varying from -1° to 1° in the AOA region, shows a nonlinear phenomenon. This phenomenon is also described in AGARD reference documents within Mach 0.9 to 1.0[1]. It is most likely that the shockwave reflects on the model, causing it to vibrate and affecting its aerodynamic behaviour.

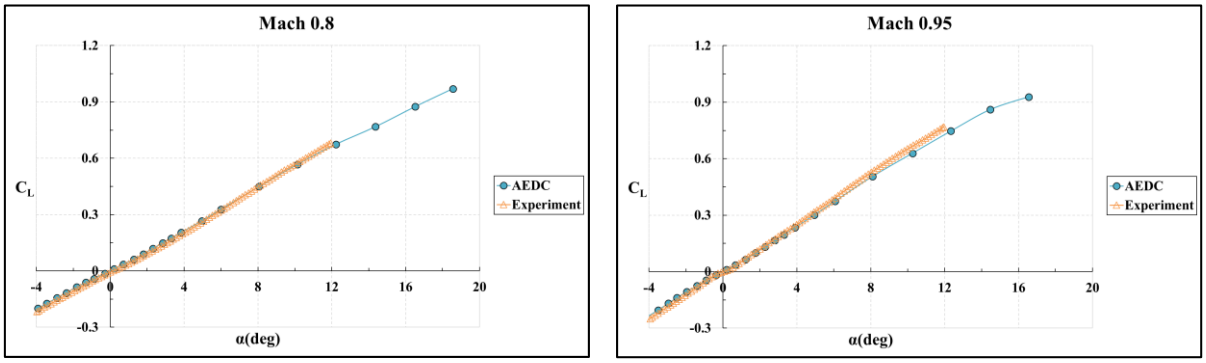

Fig. 6 Lift coefficient comparison

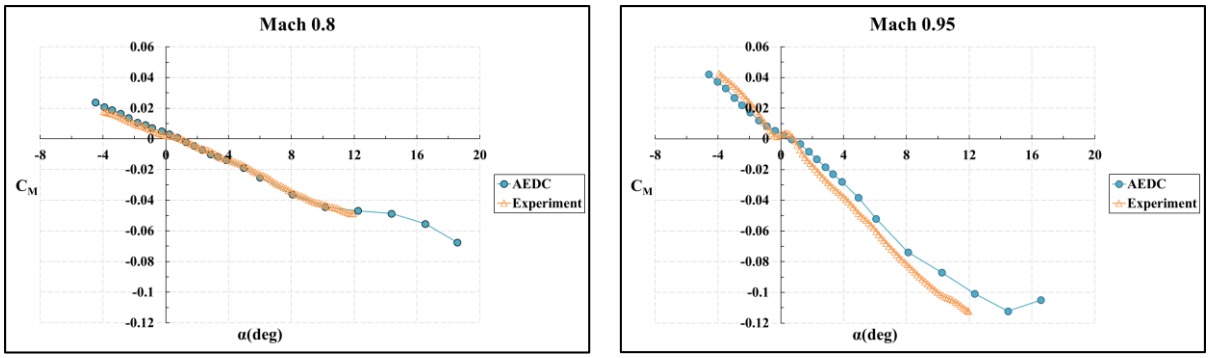

Fig. 7 Pitch moment coefficient comparison result

4.2 CFD result compared to the experiment

To study the flow phenomena, we performed steady-state CFD simulations using the same total and static pressures as the experimental tests. Before observing the flow field of the CFD simulation, we compared the aerodynamic coefficient results of the CFD simulation with those of the experiment. The analysis emphasizes the distribution trend at different Mach numbers, with data shifted and compared at a 0° angle of attack (AOA). The comparison results for the lift coefficient and pitch moment coefficient at Mach 0.8 and 0.95 are shown in Figs. 8 and 9. The relationship between the lift coefficient and AOA is linear. Although the lift coefficient is not identical to that from the experimental results and has a slightly higher slope, the trends match each other without significant differences. For the pitch moment curve (Ref. point is at 25% MAC), the relationship between the pitch moment coefficient and AOA is linear at Mach 0.8. However, the comparison result at Mach 0.95 shows a nonlinear phenomenon varying from -2° to 2° in the AOA region, and this phenomenon can be observed in both CFD simulation and experiment. It is most likely that the shockwave reflects on the model, causing it to vibrate and affecting its aerodynamic behaviour.

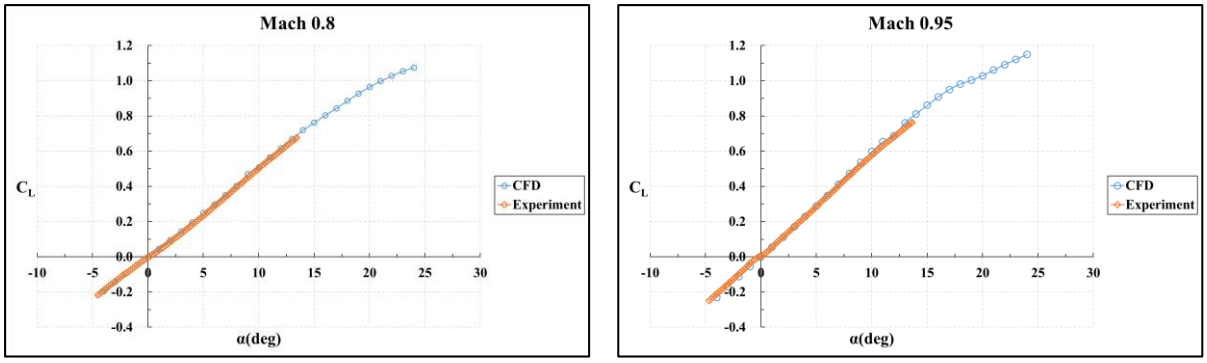

Fig. 8 Comparison of lift coefficient

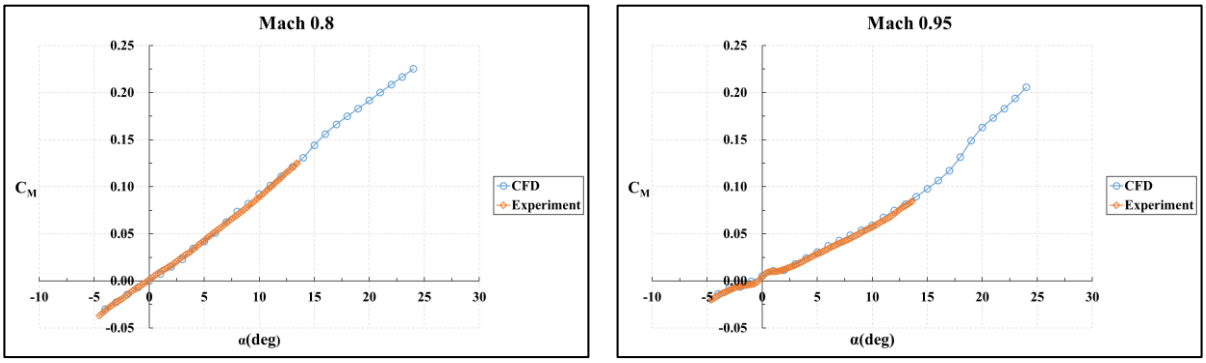

Fig. 9 Comparison of pitch moment

4.3 Flow Field Observation of CFD Simulation

In the experiment, conducting flow visualization in a high-speed wind tunnel is challenging, so we apply CFD simulation to compensate for the lack of flow visualization. According to the aerodynamic coefficient comparisons between the CFD simulations and the experiment, there are no significant differences in the trends of the coefficients. Therefore, we can examine the flow field in a CFD environment. The flow structure illustrated in Fig. 10, located 20 inches from the nose of the AGARD-B model, contains the body vortices, the two secondary vortices at the wing-body junction, and the primary and secondary leading-edge vortices, outlined by the λ2-criterion as contours.

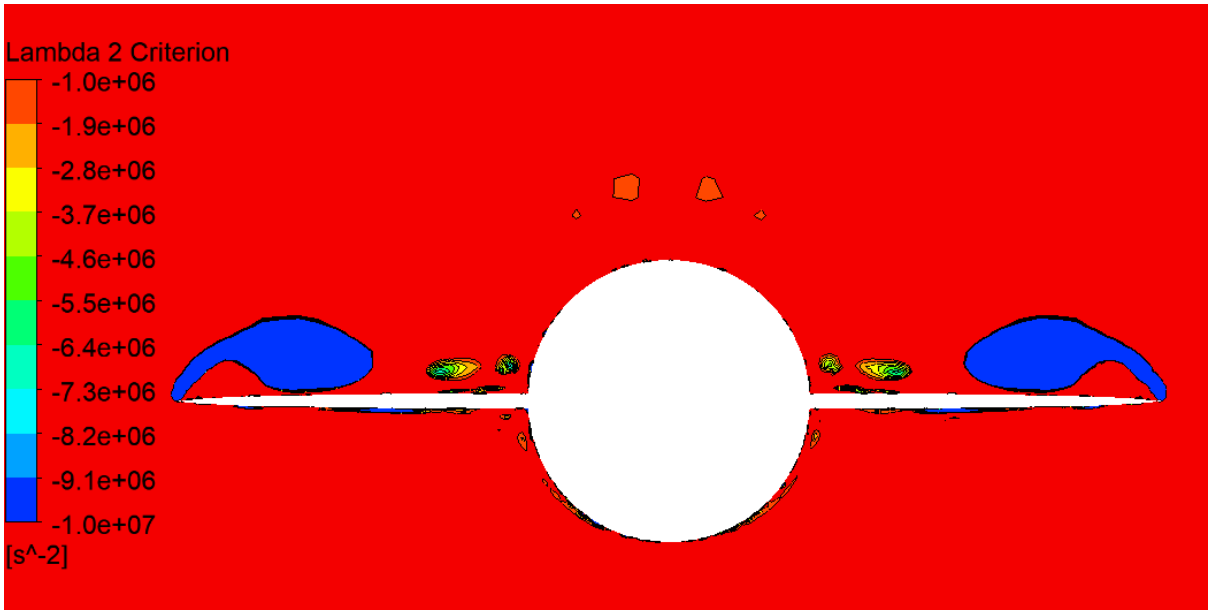

Fig. 10 Primary vortex structures for α=10° at M0.8

For the lift coefficient curve at M0.8, the CFD simulation correlates with the experimental data, indicating that vortex bursting occurs at an AOA above 13°, corresponding with the loss of lift. From the pressure coefficient plot shown in Fig. 11, the vortex bursts and the structures move closer to the body as the AOA increases to 17°. Additionally, for the Mach number plot illustrated in Fig. 12 at a location of 16 inches from the nose, vortex structures have burst, and the primary and secondary leading edge vortices are clearly generated. As the AOA increases to 17°, the location of the vortex bursting moves forward and is almost at the apex of the exposed wing.

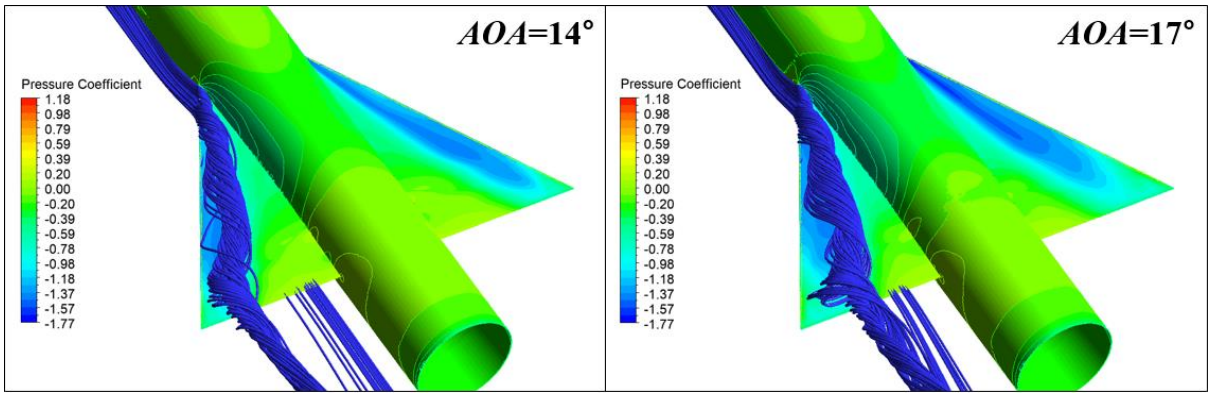

Fig. 11 Pressure contour plot at M0.8

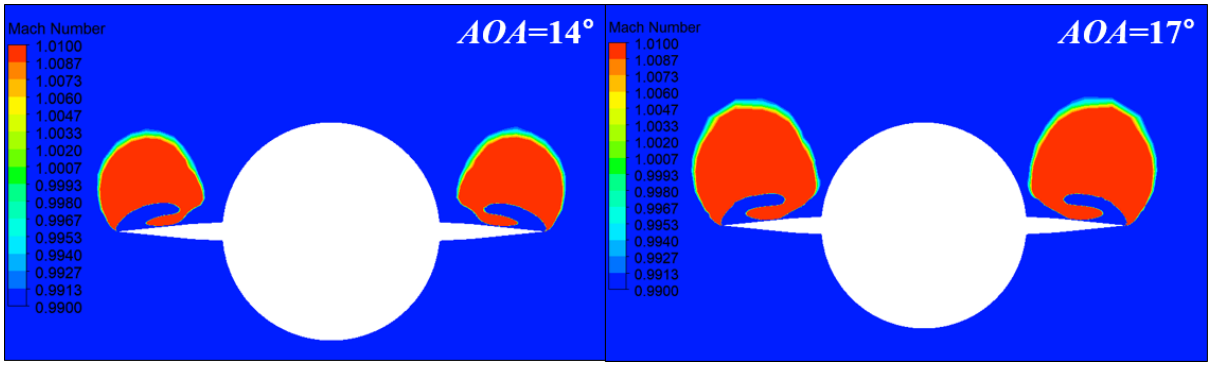

Fig. 12 Mach number contour plot at M0.8

For the lift coefficient curve at M0.95, the CFD simulation correlates with the experimental data at an AOA below 14°. From the pressure coefficient plot shown in Fig. 13, the vortex bursts and the structures move closer to the body. From the Mach number contour plot shown in Fig. 14, the body and wing upper surface are in the supersonic region, and the body vortices are more pronounced compared to Fig. 12. As a result, at M0.8, the lift begins to decrease where vortex bursting occurs, and the primary and secondary leading-edge vortices are generated. As the AOA increases to 17°, the location of the vortex bursting moves forward and is almost at the apex of the exposed wing.

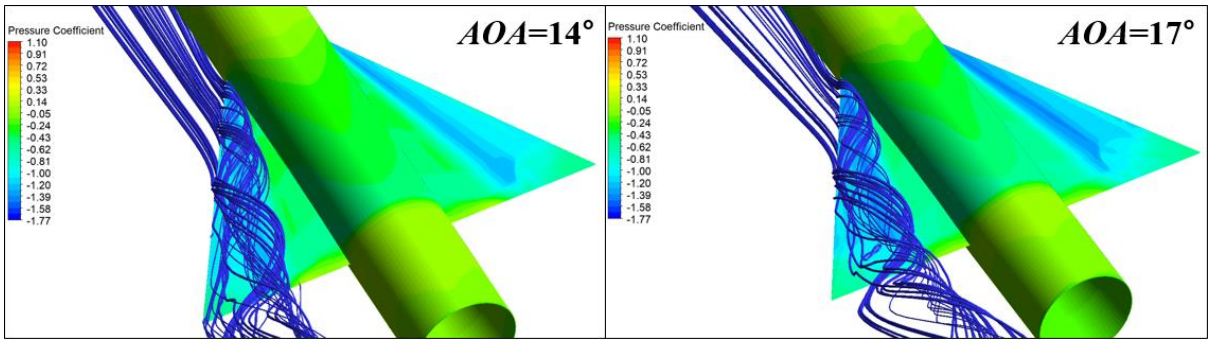

Fig. 13 Pressure contour plot at M0.95

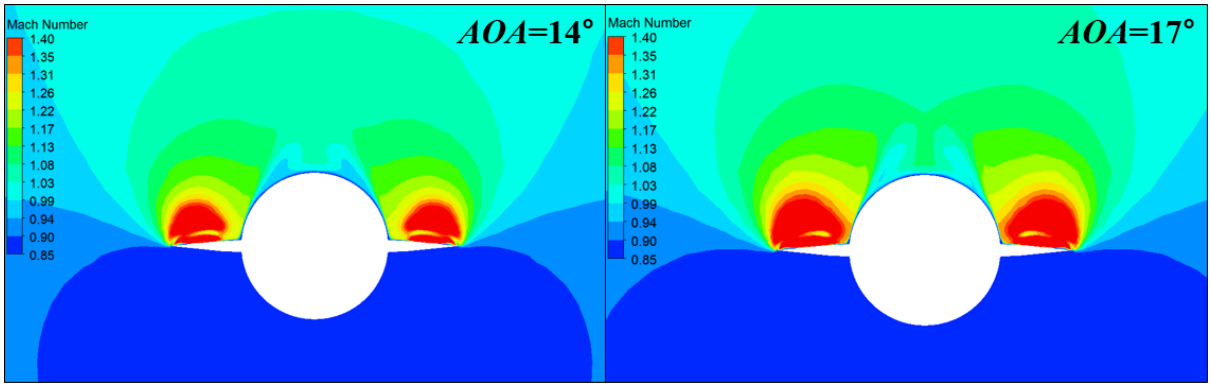

Fig. 14 Mach number contour plot at M0.95

Inspecting the flow structure when the vortex bursts, the recovery shock exists between the primary and secondary vortices. The shock appears as the flow, which is supersonic between the primary vortex and the wing upper surface, decelerates over the secondary vortex. The recovery shock only exists when the vortex bursts, and it disappears once the vortex has fully burst because the flow between the burst vortex and the wing upper surface does not exceed M1.2, as illustrated in Fig. 15.

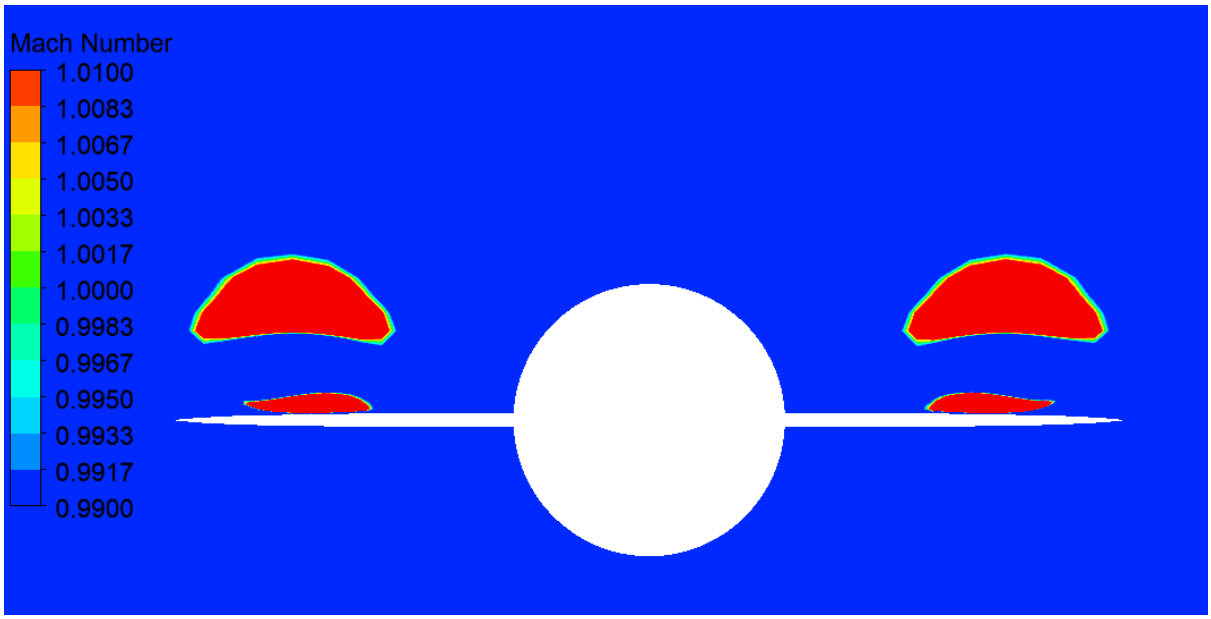

Fig. 15 Mach contours for the fully developed vortex burst at *AOA* 14°

From the comparison results of CFD simulation and experimental data, the lift and pitch moment coefficient curves of the AGARD-B model remain linear at an angle of attack (AOA) below 14°. As the AOA increases, vortex breakdown occurs. Given that the vortex breakdown occurs at a lower angle and transonic speed [10], the cause of vortex breakdown is the adverse pressure gradient of the flow, not triggered by a streamwise normal shock, because no such shock exists for this configuration. As the AOA increases, the lambda shock structure is identified between the primary vortex and the wing surface. From the simulation, the flow over the top of the vortex exceeds the speed of sound due to the upwash effect, and there is no shock on the upper side. When the AOA is above 18°, the lift reduces because of the burst vortex separating or shedding from the wing. From the streamlines on the upper surface, as shown in Fig. 16, there is a 'whorl' near the tip of the wing.

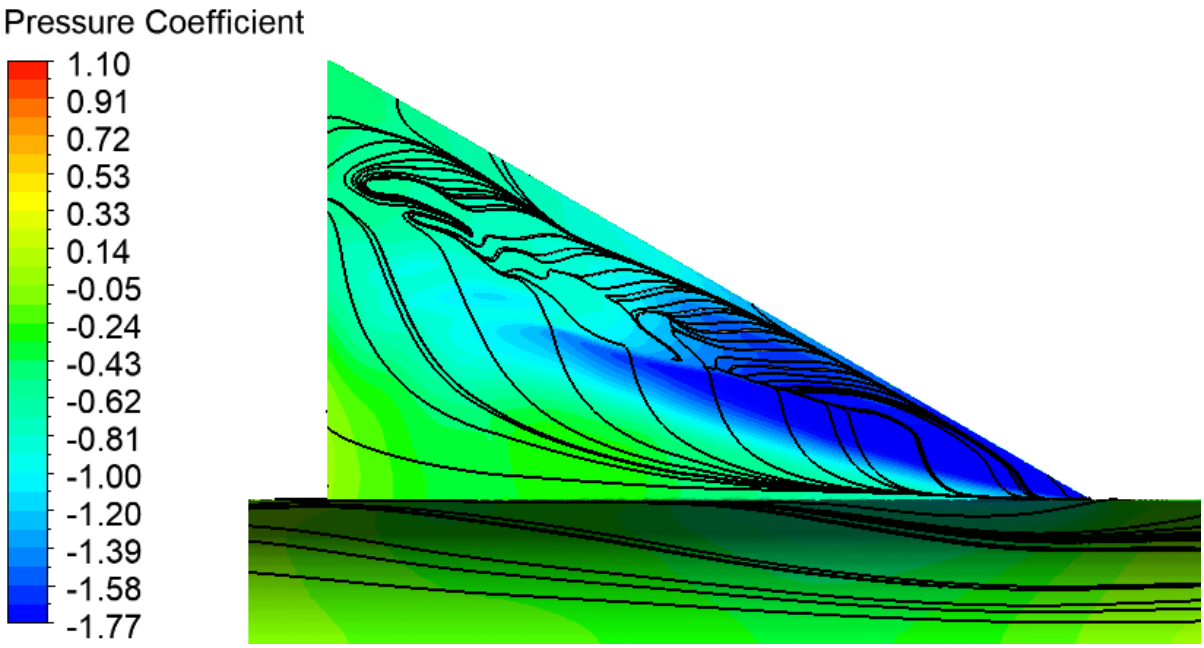

Fig. 16 On-surface streamlines at *AOA* 18°

5. Conclusion

This paper investigates the aerodynamic coefficients and compressibility effects of the AGARD-B models. The test data are compared with those from similar models tested at AEDC in the USA. The test results of the AGARD-B models show that the lift and pitch moment coefficient curves are in good agreement with the reference, confirming a high level of measurement repeatability. The comparison results of CFD and experimental data indicate that the trends of the aerodynamic coefficient curves match. Therefore, the flow structures can be observed under a reliable environment. The results show that shock structures only develop when the vortex bursts. As the angle of attack (AOA) increases over 15°, a normal or lambda shock would exist between the primary vortex, accelerating the flow and then decelerating it between the secondary vortex and the vortex sheet or leading-edge shear layer.

This study demonstrates that numerous nonlinear phenomena are observed for this configuration of a 60° biconvex wing, and the behavior of the flow over the wing across the chosen AOA range could provide a useful calibration standard for wind tunnels. From the references, there is not much experimental research on the effects where vortex bursting and vortex separation occur under this flow condition. Therefore, wind tunnel experiments need to be conducted to capture both of these phenomena.

References

1. Hills, R.: A Review of Measurements on AGARD Calibration Models. AGARDograph 64, 1961
2. C. F. Anderson: An Investigation of the Aerodynamic Characteristics of the AGARD Model B for Mach Numbers from 0.2 to 1.0. AEDC-TR-70-100, 1970
3. August F. Bromm, Jr.: Investigation of lift, drag, and pitching moment of a 60 delta-wing body combination (AGARD calibration model B) in the Langley 9-inch supersonic tunnel. Langley Aeronautical Laboratory, 1954.
4. Stanbrook, A. and Squire, L.C., Possible Types of Flow at Swept Leading Edges, Aeronautical Quarterly, Vol. XV, pp. 72-82, 1964
5. S. Tuling, B. Vallabh, M.F. Morelli: Compressibility Effects for the AGARD-B Model. 2015
6. Delery, J.M.: Aspects of Vortex Breakdown. Progress in Aerospace Sciences, Vol 30, pp. 1-59, 1994

7. Calderon, D. E., Wang, Z. and Gursul, I.: Three-dimensional measurements of vortex breakdown. Experiments in Fluids, 53(1), pp. 293-299, 2012
8. Breitsamter, C., Unsteady flow phenomena associated with leading-edge vortices, Progress in Aerospace Sciences, Vol 44, pp. 48-65, 2008
9. Mitchell, A.M. and Delery, J., Research into vortex breakdown control, Progress in Aerospace Sciences, Vol 37, pp. 385-418, 2001
10. Wentz, W.H. and Kohlman, D.L. Vortex Breakdown on Slender Sharp-Edged Wings, Journal of Aircraft, Vol 8, No 3, pp-156-161, 1971.